ELSEVIER

Journal of Nuclear Materials 307–311 (2002) 1400–1404

journal of nuclear materials

www.elsevier.com/locate/jnucmat

Kinetic features of the component interaction in the V[O]–Li[Ca] system

O.I. Yeliseyeva [a,*], V.M. Chernov [b], T.V. Tsaran [a]

[a] G.V. Karpenko Physico-Mechanical Institute NASU, L'viv 79601, Ukraine
[b] SSC RF – A.A. Bochvar Institute of Inorganic Materials, 123060 Moscow, Russia

Abstract

The interaction between vanadium alloys (V–20Ti and V–70Ti–6Cr–0.1Y) and Ca-containing liquid lithium at 700 °C up to 1500 h of exposure is analyzed using Auger spectroscopy. The kinetics of liquid metal penetration into the solid metal and a structural irregularity of the corrosion front progression are studied. A latent period is observed when lithium does not penetrate into the V–20Ti alloy. A thin protective CaO layer is formed on the alloy surface over that period, and dispersed particles of Ti_xO_y dissolve in a suboxide zone. As the latent period has passed, the protective layer disintegrates, and lithium penetrates into the alloy up to a depth of 150–200 μm in transcrystalline manner and then into deeper layers along the grain boundaries. An yttrium modification of the V–Ti matrix suppresses the Li penetration into the alloy.

1. Introduction

CaO oxide is one of those few dielectric materials stable in lithium. This oxide can be easily obtained in the same temperature range as V-based alloys are designed to operate between 400 and 700 °C. V-based alloys hold much promise for lithium systems in fusion reactors. Ca and O are easily dissolved in lithium and vanadium, respectively, and therefore the counter flows of Ca (from Li) and O (from V) can be used for in situ formation of a CaO protective layer on the solid metal–liquid metal interface. Currently, the technique of a CaO coating formation in a melt is developed [1–5], but the mechanism of the interaction of components under operating conditions in a self-healing mode is still unraveled. To find out the features of the interaction in the Li[Ca]–V–Ti[O] system the V–20Ti and V–70Ti–6Cr–0.1Y alloys as V-based candidates were selected and examined after exposure to Ca-containing lithium at 700 °C for 1500 h.

2. Experimental procedure

A 1 mm thick rolled metal sheet was used to fabricate two types of samples: $10 \times 10 \times 1$ mm^3 and $10 \times 3 \times 1$ mm^3 with a notch in the middle of each sample (for further destruction in the Auger spectrometer). The samples were annealed at 1000 °C in 10^{-4} Pa vacuum for 1 h. Later they were placed in the ampoules made of a V–1Zr–0.1C alloy. The melt (Li–0.5%Ca) was poured in an altitude chamber under purified argon atmosphere. Then, the ampoules were sealed by welding, placed in a protective steel container and hold at 700 °C. To remove the lithium remains the samples were flushed in water, butanol and alcohol. Afterwards, we investigated the phase structure of the surface layers, general concentration of nonmetallic impurities in the samples by vacuum melting and Li concentration by general chemical analysis. The interaction of the components was investigated using the Auger analysis performed on the samples exposured to liquid lithium.

3. Results

The increase of the exposure time made a little difference upon the N concentration in the alloys, though it

* Corresponding author. Tel.: +380-322 65 43 43; fax: +380-322 64 94 27.
E-mail address: fedirko@ipm.lviv.ua (O.I. Yeliseyeva).

0022-3115/02/$ - see front matter © 2002 Published by Elsevier Science B.V.
PII: S0022-3115(02)00989-3

had an effect upon the C concentration (Table 1). The Li and O content in the samples increased only after 500 and 1500 h exposure. Under the identical conditions of the corrosion test the Li concentration in the V–70Ti–6Cr–0.1Y samples was 50% less of that in V–20Ti samples.

The vanadium lines dominate in all X-ray diffractograms obtained from the surface of the samples after exposure to lithium. CaO lines are observed after 50 and 250 h of exposure. After the more prolonged exposure we observe the broadened and less intensive peaks and therefore, a phase identification is complicated. The cracks appearing on the surface of the fractured samples are seen in Fig. 1(a). It spreads in a transcrystalline manner in a depth range of 150–200 μm and forms a typical brittle fracture pattern (Fig. 1(b)). In the deeper layers the sample is fractured along the grain boundaries (Fig. 1(c)). The mixed destruction can be rarely traced. The morphology of the grain surface in a zone of the intercrystalline fracture presumes the presence of some corrosion products promoting the sample's fracture.

In order to identify this product the Auger analysis (Fig. 2) was carried out from several segments of the fractured surface (Fig. 1(a)), as well as from the cross-section of the specimen. The content of each component in a spectrum was determined from the ratio of the line intensity of a particular component (I_X) to the intensity of the vanadium line (I_V). The Auger analysis enables us to estimate the change of the elements' concentration (I_X/I_V) on the cross-section of a sample taking into

Table 1
Content of Li and nonmetallic impurities in V alloys exposed to Li–0.5%Ca at 700 °C

Alloy	Time of exposure (h)	Content of elements (mass %)			
		O	N	C	Li
V–20Ti	0	0.035	0.008	0.020	0
	50	0.030	–	–	0
	250	0.038	–	–	0
	500	0.060	–	–	0.85
	1500	0.080	0.010	0.035	0.88
V–70Ti–6Cr–0.1Y	0	0.040	0.030	0.020	0
	500	0.080	0.030		0.49
	1500	0.100	0.031	0.078	0.49

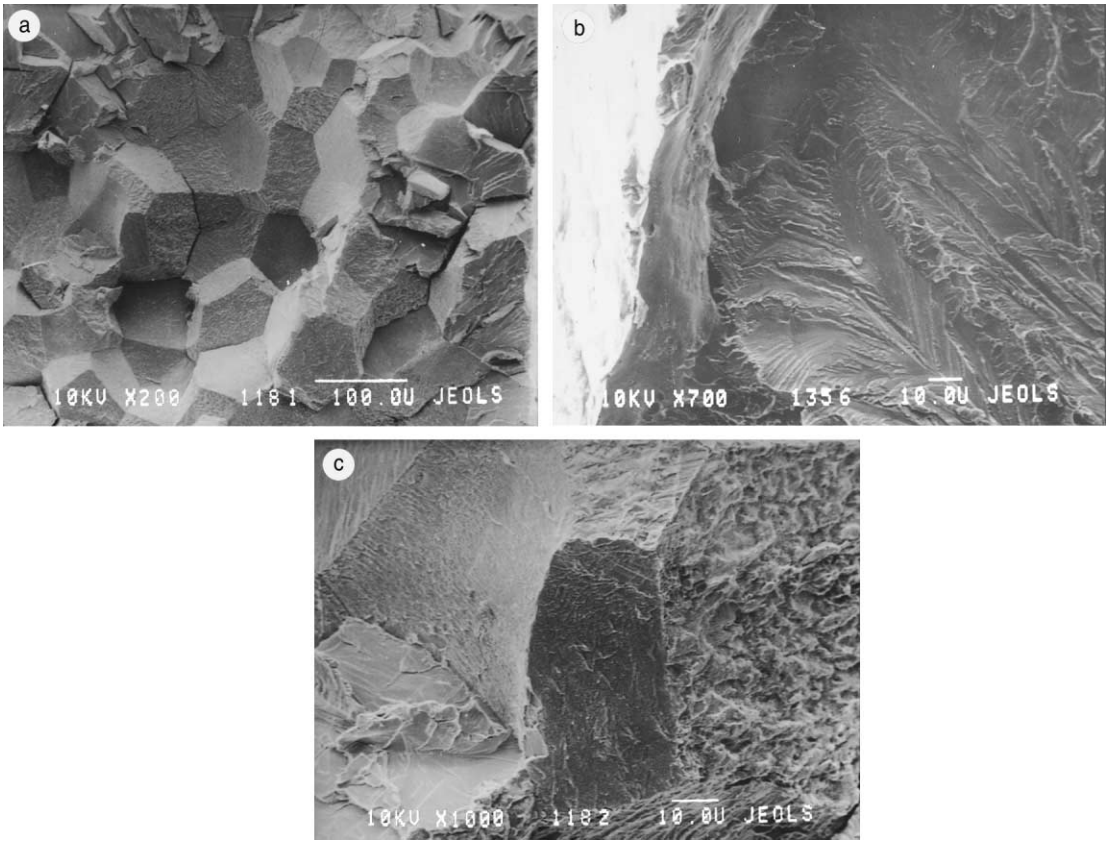

Fig. 1. Surfaces of a V–20Ti alloy sample (a–c) after exposure to a Li–0.5%Ca environment at 700 °C for 500 h.

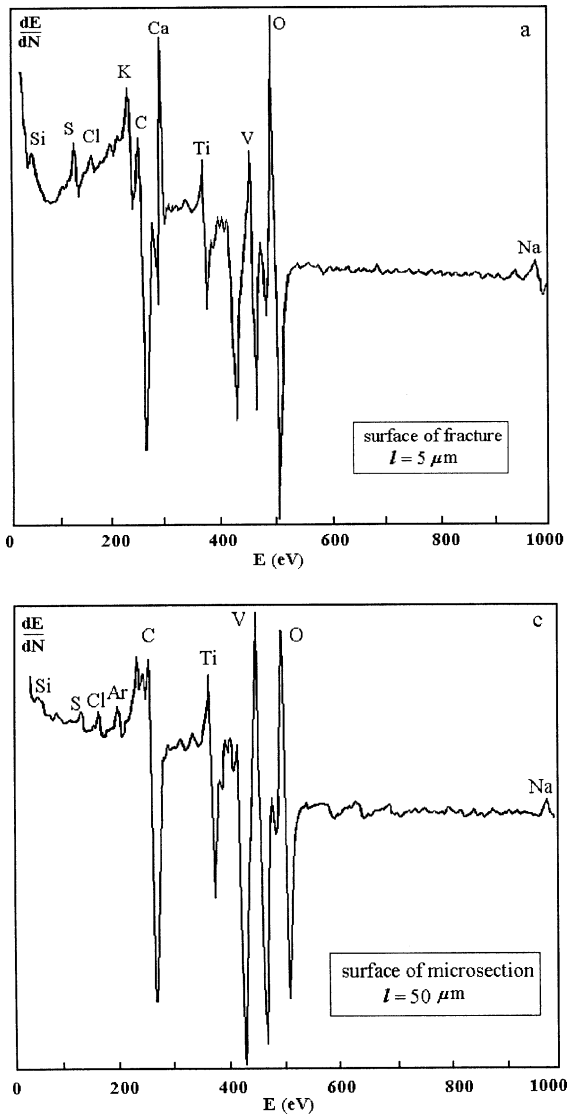

Fig. 2. Typical Auger spectra of the fractured surface (a) and microsection surface (c) of V–20Ti alloy samples exposed to Li–0.5%Ca. *l* is the distance from a lateral area of the sample to the scanning point.

account their distributions between the grain bodies and boundaries (Fig. 3(a)). The low energy of the lithium Auger electrons and the coincidence of the Li and V lines do not allow the lithium in the alloy to be revealed. However, the lines of the lithium typical admixtures (A), such as Ca, K, Na, Cl, P, Si, S, imply the lithium penetration into the alloy, whereas the chemical analysis data directly show the increase of the lithium concentration in the samples up to 0.85 wt% after 500 h of exposure (Fig. 2 and Table 1).

The analysis of the distribution of the elements in the V–20Ti alloy after its contact with lithium, and the information on the content of the elements both in the grain bodies and on grain boundaries is given in Fig. 3.

Surface ($l = 0$): A very thin solid film ($\simeq$1 μm) appears on the samples exposed to liquid Li for 500 h. The film is fairly adherent to the thick (10–12 μm) fragile underlying layer (Fig. 1(b)). The O and Ca lines are the most intensive in the spectrum of this layer (Fig. 2(a)). Apparently, the surface layer consists of CaO. Amorphous carbon occur in this layer as is transferred from the ampoule material.

Zone of transcrystalline fracture ($0 < l < 200$ μm): The concentrations of O and Ti inside the grain bodies and on grain boundaries are approximately the same. The general intensity of the admixtures lines (A) is lower than that in the surface layer. Nevertheless, each kind of admixture in lithium, except Ca, is clearly observed just inside of the grain bodies and on the grain boundaries. Calcium does not penetrate deeper than 10–15 μm. Carbon occurs in the given zone, but far less than on the surface. The intensity of the carbon line on the grain boundaries is far lower than that inside the grain bodies, and carbon forms carbides (MeC).

Zone of intercrystalline fracture ($l > 200$ μm): The concentrations of O and Ti are twice less in comparison to the previous zone. These elements are much more densely located on grain boundaries than inside the grain bodies. Also, no admixtures (A) are revealed inside the grain bodies. At the same time these impurities are clearly observed on the grain boundaries, i.e. Li penetrates into the alloy in an intercrystalline manner (Fig. 3).

Thus, after the exposure to Ca-containing liquid lithium at 700 °C:

- the calcium-enriched thick layer (10–15 μm) is formed on the sample surface;
- there is a latent period when lithium does not penetrate into the V–20Ti alloy;
- the typical for the initial state of the V–20Ti alloy accumulation of O and Ti on the grain boundaries comes to naught in the transcrystalline fracture zone (up to 200 μm in depth), though in the deeper layers it remains unchanged;
- the lithium penetrates into the alloy both through the grain bodies and along grain boundaries in the transcrystalline fracture zone, and only along grain boundaries in the deeper layers.

4. Discussion

The identified kinetic features of the interaction and examination of the sample exposed to the lithium melt prove the step-by-step character of the interaction between the components in the V–Ti[O]–Li[Ca] system.

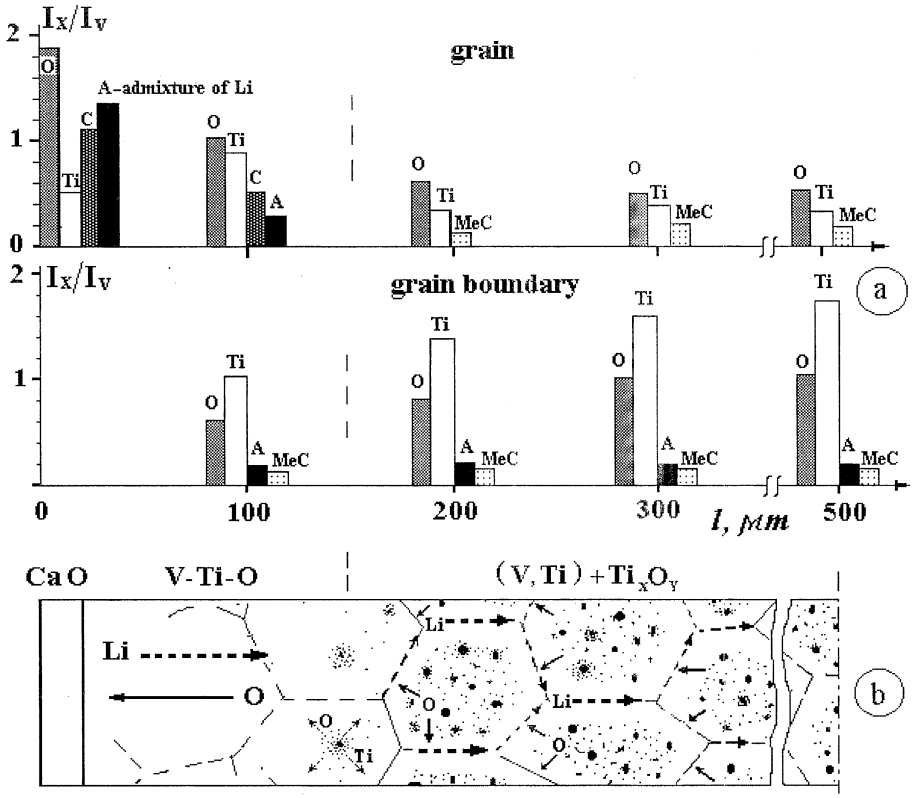

Fig. 3. (a) Relative content of the elements (I_X/I_V) along the cross-section of the V–20Ti alloy sample exposed to the Li–0.5%Ca melt at 700 °C for 500 h; I_X – intensity of the line of the particular component in the Auger spectra and I_V – intensity of the vanadium line, (b) scheme of the alloy structure formed after the exposure, *grain* – content of elements inside grain body; *grain boundary* – content of elements on grain boundaries; A – admixture of Li – general content of lithium impurities (Ca, K, Si, S, P, Cl, Na); MeC – carbon content in carbides.

The CaO layer forms initially on the surface of the solid metal due to the counter flows of O from V and Ca from Li. The mechanism of CaO oxidation usually is based on the primary diffusion of the Ca cations, but it cannot be implemented in the given system, as the solid metal prevents the oxide growth. Probably, the growth takes place at a deficit of oxygen, as its delivery is limited by the diffusion in a solid phase, while calcium is delivered from a liquid phase. Consequently, an excess of the anion defects appears in CaO and ensures the oxygen diffusion through the oxide layer. While the layer is growing the CaO structure improves, gains protective properties and the oxygen flux from the matrix to the reaction zone slows down.

The growing of the external oxide layer is accompanied by a rapid decrease of the oxygen concentration in the subsurface layer as well as by the imbalance between the solid solution and Ti_xO_y particles. This is confirmed by a decrease of the density of the particles as well as by the migration of the released grain boundaries in a suboxide layer. The Ti_xO_y particles are dissolved near the interface and on the grain boundaries, and the Ti-enriched zones appear due to low diffusive mobility of titanium. The higher the titanium content in a refractory metal, the higher is the oxygen solubility and the stronger is the suboxide α'-phase stability [6,7].

An α'-phase can be formed in the V-matrix at sites of selective dissolution of the particles and, as a result the Li penetrates into the alloy. Such penetration occurs due to a solid phase reaction according to the mechanism of the reactive diffusion with formation of the ternary oxide $L_xMe_yO_z$, where L is a liquid metal component (Ca or Li), and Me is a solid metal (Ti or V) [8]. Calcium as an element with a higher affinity to oxygen first of all forms an external oxide layer and penetrates into the subsurface layer of the solid metal. The reserve of calcium in our experiment is gradually exhausted in a closed ampoule space. According to the Auger spectroscopy data the calcium penetrates into the matrix up to a depth of 10–15 μm. Lithium follows after calcium, though it

penetrates deeper into the V-matrix: first in a frontal manner and later selectively along the grain boundaries. Such irregular progression of lithium is a result of the selective disintegration of the Ti_xO_y oxides. The particles near the intense drain of oxygen (the solid metal–liquid metal interface) disintegrate first. Therefore, the disintegration conditions of the oxides located on the grain boundaries and in the grain bodies are the same. In the deeper layers (>200 μm) the particles located on the grain boundaries basically disintegrate. Li is advanced selectively only in the areas with an increased concentration of O and Ti, that is where the α′-phase is formed.

The histograms of the element distributions through the specimen were plotted on the basis of the Auger analysis data in Fig. 3(a). The upper histogram was plotted taking into account the distributions of the elements in the body of grains and the bottom one taking into account the distributions of the elements on the grain boundaries. Also, for better clearness and understanding of the results of this complex analysis the generalized scheme of the alloy structure formed after exposure is presented in Fig. 3(b). The scheme and histograms are dependent mutually and are presented as a function of the distance from the specimen surface (axis *l*).

Under the considered experimental conditions ($T =$ 700 °C; Li–0.5Ca) the protective CaO layer remains on the surface of the V–20Ti alloy for 250–500 h. The lack of Ca in the melt causes the layer degradation. The presence of yttrium in the V–70Ti–6Cr–0.1Y alloy increases its resistance to the lithium penetration. In comparison to vanadium and titanium, yttrium has a higher affinity to oxygen and binds some oxygen to the oxides stable in a lithium environment. This means why the lithium penetration into the V alloy is limited.

5. Conclusions

Under high temperature (700 °C) and long-term (1500 h) contact of the V–20Ti alloy with Ca-containing lithium (Li–0.5%Ca), the CaO oxide layer,is formed on the alloy surface. This layer keeps its protective properties up to 500 h, which causes the existence of a latent period, when liquid lithium does not penetrate into the alloy (Table 1). After longer exposures the layer is dissipated because of the lack of calcium in the melt, and lithium penetrates into the alloy. Its concentration in the alloy grows up to 0.88 wt%. The lithium is advanced into the solid metal at first in a frontal manner (at a depth of 200 μm), and later along the grain boundaries enriched with titanium and oxygen.

References

[1] V.N. Mikhailov, V.A. Evtikhin, I.E. Lyublinski, A.N. Vertkov, A.M. Chumanov, Lithium for Fusion Reactors and Space Nuclear Power Systems of XXI century, Energoatomizdat, Moscow, 1999, 528 p., in Russian.
[2] S. Malang, H.U. Borgstedt, E.H. Farnum, K. Natesan, I.V. Vitkovski, Fus. Eng. Des. 27 (1995) 570.
[3] J.H. Park, T. Domenico, G. Dragel, R. Clark, Fus. Eng. Des. 27 (1995) 682.
[4] K. Natesan, M. Uz, S. Wieder, Organisation Semiannual Progress Report for Period Ending June 30, 1999, p. 57.
[5] J.-H. Park, T.F. Kassner, J. Nucl. Mater. 233–237 (1996) 476.
[6] J.R. Distefano, J.W. Hendricks, Nucl. Technol. 110 (1995) 145.
[7] I.I. Kornilov, V.M. Dekanenko, V.V. Vavilova, Inorg. Mater. (1) (1973) 1964, in Russian.
[8] A.G. Arakelov, L.N. Galkin, V.V. Vavilova, A.A. Gekov, Prot. Met. 17 (2) (1981) 233, in Russian.